

Effects of magnetic fields on wave propagation in dense laser-produced plasmas

R.A. CAIRNS AND B. RAU*

School of Mathematical and Computational Sciences, University of St Andrews, St Andrews, Fife KY16 9SS, UK

(RECEIVED 25 May 1999; ACCEPTED 14 June 1999)

Abstract

Simulations of the interaction of very intense short pulse lasers with solid density plasmas have indicated that there may be very high magnetic fields and electron temperatures in the vicinity of the focal spot. We investigate the propagation of an incident electromagnetic wave under these conditions, both analytically and by means of a particle code, and show that the evanescence length of the wave field in a highly overdense plasma may be much greater than is usually supposed. This effect could be important in understanding the penetration of energy into the overdense region and the particle heating and acceleration which takes place there.

1. INTRODUCTION

The interaction of very intense short laser pulses with solid density targets is a subject of considerable interest at present (Wilks & Kruer, 1997), stimulated by the development of lasers which can produce pulses with focused intensities of 10^{19} W/cm² or more and duration of the order of 100 ps (Perry & Mourou, 1994). The interest also arises from the possible application of such pulses to the fast ignitor, a possible means of reducing the energy requirement for ignition of laser fusion targets (Tabak *et al.*, 1994). The recent experimental observation of laser light transmission through highly overdense plasma (Giulietti *et al.*, 1997; Fuchs *et al.*, 1998) supports the use of laser pulses as candidates for the energy deposit onto these targets.

Simulations and theoretical investigations of such systems indicate that in the vicinity of the focal spot the fast electrons produced near the plasma surface may form beams penetrating the target and that the currents resulting from such beams may generate extremely high magnetic fields, of the order of hundreds of mega Gauss (Pegoraro *et al.*, 1997; Sudan, 1993; Wilks *et al.*, 1988). At the same time, the plasma electrons near the surface reach temperatures of the order of hundreds of keV (Beg *et al.*, 1996; Wilks *et al.*, 1992). The purpose of this paper is to point out that such conditions may have an important effect on the behavior of the wave field inside the plasma, increasing the evanescence length in a

highly overdense plasma to a value many times greater than the classical skin depth c/ω_{pe} , c being the speed of light and ω_{pe} the Langmuir frequency of the plasma. In fact, we will show that the evanescence length of a hot, strongly magnetized, and highly overdense plasma becomes larger than any of the usual estimates of anomalous skin depth (Matte & Aguenou, 1992), or those expected from cold, magnetized plasma theory (Teychenné *et al.*, 1998) (see Fig. 1). This could have important consequences for the penetration of the wave into the plasma and the absorption of energy in the overdense region. Teychenné *et al.* (1998) pointed out that the cold plasma cutoff for the X-mode is at a density above critical. However, to make a highly overdense plasma transparent by this mechanism requires enormous magnetic fields. We show that thermal effects are important in enhancing transmission at much lower fields.

The theory which we present is based on linear theory, with the role of high intensity laser radiation simply to provide the necessary temperatures and magnetic fields. In reality, of course, the system is highly nonlinear. However, we take the view that linear wave propagation theory should provide a first approximation to the behavior of the wave and certainly must be understood before nonlinear effects are included. We use the weakly relativistic dielectric tensor elements (Shkarofsky, 1966), which are well-known in the theory of low density plasmas and are widely used in space physics and tokamak physics, providing well-verified descriptions of, for example, cyclotron emission and absorption (Bornatici *et al.*, 1983). However, they are less well known in the laser-plasma community and, so far as we know, no one has looked in detail at the effect of high temperature and magnetic field in overdense plasmas.

*Present address: Helsinki University of Technology, Department of Engineering Physics and Mathematics, FIN-02015 HUT, Finland

Address correspondence and reprint requests to: B. Rau, Helsinki University of Technology, Department of Engineering Physics and Mathematics, PO Box 2200, FIN-02015 HUT, Finland. E-mail: bernhard.rau@hut.fi

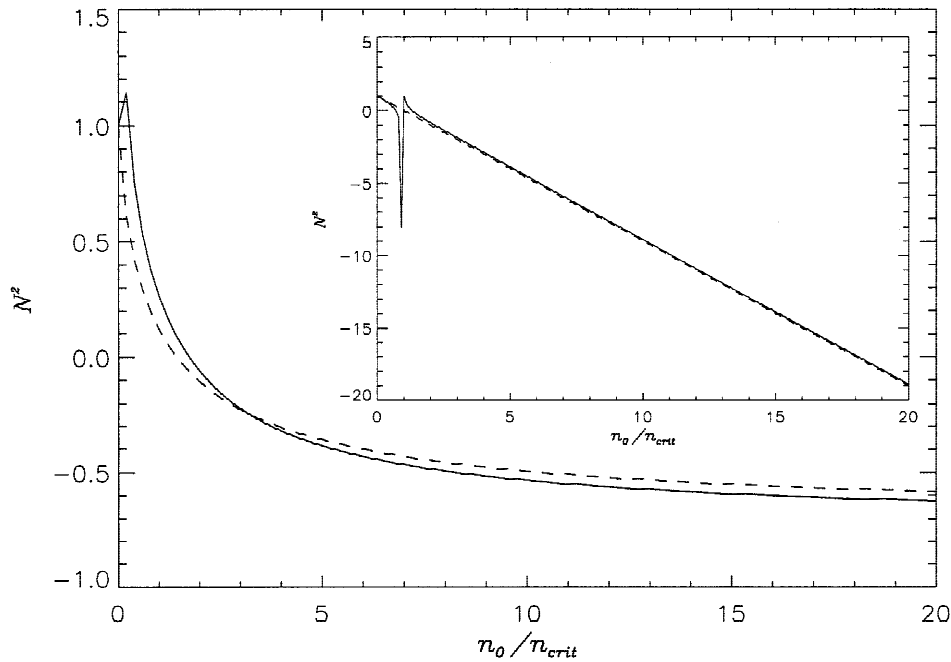


Fig. 1. N^2 as a function of normalized plasma density n_0/n_{crit} for $\omega_{ce}/\omega = 0.3$ and $T_e = 100$ keV. The result for the X-mode is shown in the solid, for the O-mode in the dashed line. N^2 approaches 1 for the X- and O-mode as the density is reduced to zero. The values becomes very different from the cold plasma cases (inset) as the plasma density increases. Inset: The linear dispersion relations for the X- (solid) and O-modes (dashed line) of a cold plasma for comparison [see Eq. (9)]. Note the different range of N^2 .

The tensor elements which we use are based on an expansion which assumes the quantity $\mu = m_e c^2/T_e$, m_e being the electron’s mass, to be large. This implies that the electron thermal energy T_e is small compared with its rest energy which is a good approximation except, possibly, for very high intensity pulses. Exact relativistic dielectric tensor elements are available (Shkarofsky, 1966) but are less easy to handle than the weakly relativistic versions. We also restrict our attention to propagation perpendicular to the magnetic field. This is the simplest case to deal with theoretically and also, since the magnetic field forms a torus around the focal spot, it seems to be the most appropriate to the geometry of the problem.

The refractive index

$$N = kc/\omega \tag{1}$$

is determined by

$$\epsilon_{\perp}(\epsilon_{\perp} - N^2) - \epsilon_{xy}^2 = 0 \tag{2}$$

for the extraordinary (X) mode and by

$$N^2 - \epsilon_{\parallel} = 0. \tag{3}$$

for the ordinary (O) mode.

where

- k = wavenumber along the direction of interest
- ω = frequency of the electromagnetic wave
- ϵ = elements of the dielectric tensor are denoted as ϵ .

We consider propagation perpendicular to the magnetic field and use weakly relativistic dispersion relations, valid for $T_e/mc^2 \ll 1$. Defining the electron cyclotron frequency $\omega_{ce} = eB/(m_e c)$ where B denotes the magnetic field strength and $-e$ the electron charge, along with

$$\lambda = \frac{N^2 \omega^2}{\mu \omega_{ce}^2}, \tag{4}$$

the dielectric tensor elements which appear in these formulae are defined as follows:

$$\begin{aligned} \epsilon_{\perp} &= 1 - \frac{\omega_{pe}^2}{\omega^2} \mu \sum_{n=1}^{\infty} \frac{n^2 \lambda^{n-1}}{2^n n!} F_{n+(3/2)}^+ \\ \epsilon_{xy} &= \frac{\omega_{pe}^2}{\omega^2} \mu \sum_{n=1}^{\infty} \frac{n^2 \lambda^{n-1}}{2^n n!} F_{n+(3/2)}^- \\ \epsilon_{\parallel} &= 1 - \frac{\omega_{pe}^2}{\omega^2} \mu \left\{ F_{5/2}(z_0) + \sum_{n=1}^{\infty} \frac{n^2 \lambda^n}{2^n n!} F_{n+(5/2)}^+ \right\} \end{aligned} \tag{5}$$

with the Dnestrovsky functions

$$F_q(z) = -i \int_0^\infty \frac{d\tau}{(1-i\tau)^q} e^{iz\tau},$$

$$F_{n\pm q} = F_{n+q}(z_n) \pm F_{n+q}(z_{-n}), \tag{6}$$

for half integer q and the argument $z_n = \mu(1 - n\omega_{ce}/\omega)$.

The F_q functions can be expressed in terms of the plasma dispersion function Z as follows

$$F_q(z) = \frac{i\sqrt{\pi}}{\Gamma(q)} (-z)^{q-3/2} \sqrt{z} Z(i\sqrt{z})$$

$$+ \sum_{\nu=0}^{q-(3/2)} (-z)^\nu \frac{\Gamma(q-1-\nu)}{\Gamma(q)}$$

$$= -\frac{i\pi}{\Gamma(q)} (-z)^{q-3/2} z^{1/2} e^z \operatorname{erfc}(z^{1/2})$$

$$+ \sum_{\nu=0}^{q-(3/2)} (-z)^\nu \frac{\Gamma(q-1-\nu)}{\Gamma(q)}. \tag{7}$$

These expressions, however, are not suitable for calculation for large z , since the polynomial is canceled by the leading terms in the asymptotic expansion of the first part and the whole thing goes as $1/z$. Successive integration by parts of the complementary error function in Eq. (7) followed by a change of variable leads to the following more suitable form

$$F_q(z) = \begin{cases} 2 \int_1^\infty \frac{\exp[z(1-u^2)]}{u^{2q-1}} du, & z \geq 0 \\ 2 \int_0^\infty \frac{\exp[z(2iu+u^2)]}{(u+i)^{2q-1}} du, & z < 0 \end{cases} \tag{8}$$

For the purpose of our numerical calculations we truncated the series in Eq. (5) after 40 terms, checking that this gave accurate results for all the parameters we considered. Since the equation for the refractive index is then a high order polynomial equation it has, of course, multiple roots and a numerical root finding routine will converge to different values depending on the initial estimate of the root. In order to choose a definite root we have adopted the procedure of following that branch which connects smoothly to the vacuum value, $N = 1$. This is easily done by calculating the values of N in an increasing density profile.

Some values of N^2 are shown in Figure 1. It will be immediately obvious that, as we move into the high density regime, the value of N^2 is quite different from the values

$$N_O^2 = 1 - \frac{\omega_{pe}^2}{\omega^2} \quad \text{and} \quad N_X^2 = 1 - \frac{\omega_{pe}^2}{\omega^2} \frac{\omega^2 - \omega_{pe}^2}{\omega^2 - \omega_{pe}^2 - \omega_{ce}^2} \tag{9}$$

for the cold plasma O - and X -modes (see inset of Fig. 1). The reason for this is easily seen if we consider the O -mode, which has the simpler dispersion relation. The dielectric tensor element ϵ_{11} is a series in N^2 , so if we just consider the first two terms we get an equation of the form

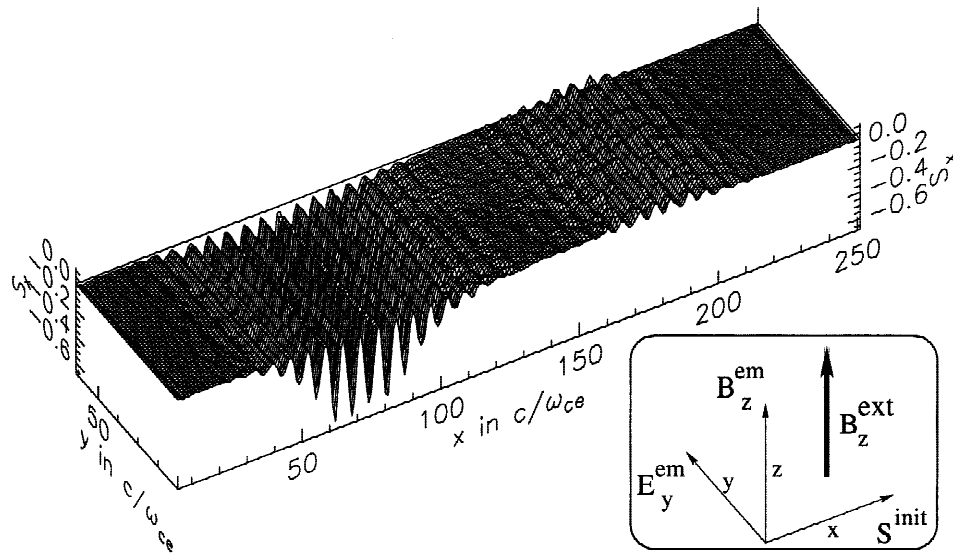


Fig. 2. The electromagnetic energy flux S_x along the x -direction. The slab of plasma is located between $123.35 c/\omega_{pe}$ and $132.15 c/\omega_{pe}$. The amplitude of the initial energy flux was normalized to 1. While about 70% of the electromagnetic wave is reflected by the four times overdense plasma, almost 12% is transmitted and about 18% is absorbed. Inset: An external magnetic field B^{ext} is applied along the z -axis, while the electric field E^{em} of the wave points along the y -direction (X -mode). The initial wave is propagating along the x -axis, that is, the initial Poynting flux S_x^{init} is positive.

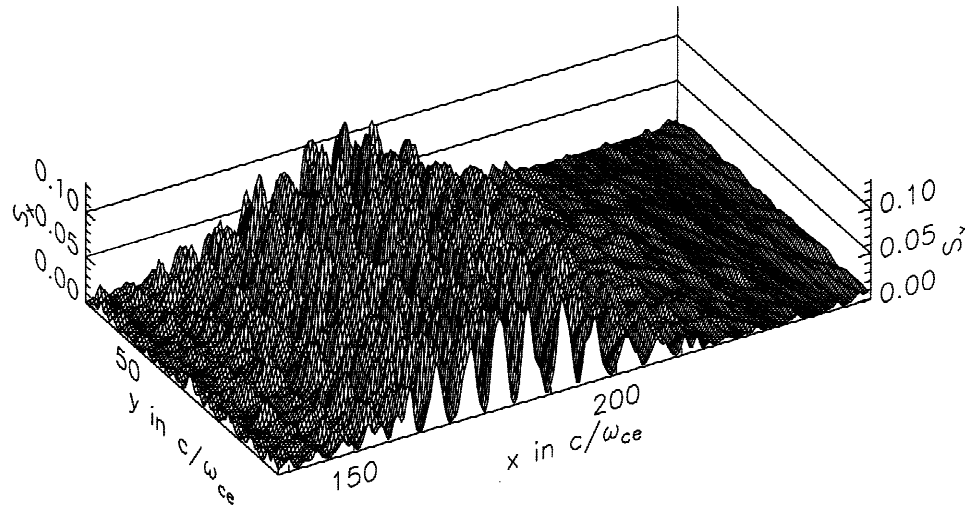


Fig. 3. Blowup of Figure 2 of the region behind the plasma slab. The transmitted electromagnetic radiation has the same Gaussian shape and the same frequency as the initial pulse. About 12% of the initial energy flux is transmitted through the slab of overdense plasma.

$$N^2 = 1 - \frac{\omega_{pe}^2}{\omega^2} (a + bN^2).$$

For moderate electron temperatures, a close to 1, and small b , we get a result close to Eq. (9). However, b increases with temperature and if, in addition to high temperature, we have a high density so that $\omega_{pe}^2/\omega^2 \gg 1$, the solution of Eq. (3) approaches

$$N^2 = -\frac{a}{b}$$

instead of Eq. (9). In particular, in contrast to the low temperature case in Eq. (9), N^2 becomes independent of the plasma density. At large ω_{pe}^2/ω^2 , equating the first two terms in the series expansion of ϵ_{ii} in this fashion gives a reasonable estimate for N^2 but generally more terms need to be included for an accurate result. For example, this crude approximation gives $N^2 \approx -0.49$ for the O -mode with the parameters of Figure 1, a value which matches quite well the asymptotic behavior for high density.

We have investigated this effect with the help of a particle code. The numerical simulations were carried out using a fully relativistic, fully electromagnetic, 2D3V PIC code [two spatial and three velocity dimensions particle in cell code, see Tajima (1989) or Birdsall & Langdon (1991)]. For our numerical investigations, we initialized a nonrelativistically weak electromagnetic pulse with a maximum amplitude of $E_{max} = 0.1m_e\omega c/e$ from a vacuum region ahead of a slab of preionized plasma in thermal equilibrium and let it evolve towards this slab at normal incidence. The pulse had a Gaussian shape along the direction of propagation with a full width at half maximum of about three wavelengths of the electromagnetic radiation λ_{em} (see Fig. 2, 4, and 5) and was uniform along the perpendicular spatial direction. We choose

periodic boundary conditions along both spatial directions on a grid of about $20\lambda_{em} \times 5\lambda_{em}$. An external magnetic field directed perpendicularly to the direction of the laser pulse propagation and to the laser light polarization (X -mode) was applied uniformly throughout the simulation region. The plasma density n was chosen to be only four times overdense ($n/n_{crit} = 4$) in order to keep the simulation box at a reasonable size. Furthermore, the plasma thickness was fixed at 0.7 of a laser wavelength to ensure a (theoretically predicted) transmission of the laser light at intensities well above the noise level while keeping the amplitude of the laser pulse within the linear regime. In order to achieve qualitative agreement with our theory, the typical Larmor radius of the plasma electrons has to be small compared to the longitudinal size of the plasma slab. Since we choose plasma electron temperatures of up to 125 keV, the applied external magnetic field was as large as $B^{ext} = m_e\omega c/e$ for some of the runs. Finally, in order to gain a relatively good representation of a hot, Maxwellian plasma electron distribution, we used up to 355 macro electrons per cell in our simulations. Furthermore, the electrons were initialized at a longitudinal position such as to closely match a density distribution determined by

$$\frac{\partial^2}{\partial x^2} \Phi(x) = -4\pi e[n_i(x) - n_{e0}e^{e\Phi(x)/T_e}].$$

Here, the ion density $n_i(x) = n_{i0}$ along the longitudinal extent of the slab of plasma Δ_p and zero everywhere else and $\Phi(x)$ is the electrostatic potential due to the thermally induced charge separation along the longitudinal direction. n_{e0} , the electron density at the center of the slab, is determined by the requirement of an overall charge neutrality, that is, by $n_{i0}\Delta_p = n_{e0}\int_{-\infty}^{\infty} \exp[e\Phi(x)/T_e] dx$. The ions were treated as an immobile source of background charges.

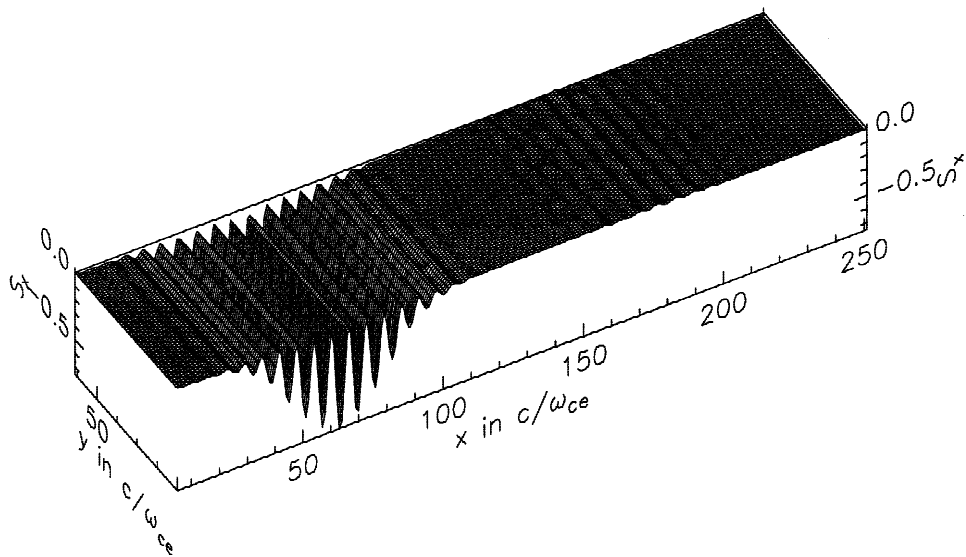


Fig. 4. Results of the same run as shown in Figure 2 but without the external magnetic field. The transmission of the electromagnetic energy flux is drastically reduced to about 2%.

We ran the code for several runs with different initial conditions for the electron temperature and the external magnetic field strength B^{ext} . The ion distribution and the laser pulse parameters remained unchanged, the electron distribution changed according to the plasma temperature. Figure 2 and Figure 3 show the result for the propagation of an electromagnetic wave through a hot (125 keV), magnetized ($\omega_{ce} = \omega_{pe}$) slab of plasma. The transmission of energy flux

through the plasma in this simulation was about 12%, compared to about 8% determined by our analytical model, and compared to about 10^{-7} for the cold, unmagnetized case with the same plasma thickness. In Figure 4, the case of transmission through hot (125 keV), unmagnetized ($\omega_{ce} = 0$) plasma is shown for comparison. Since the temperature was chosen to be the same, the electron distribution in both cases was identical. The transmission of the electromagnetic

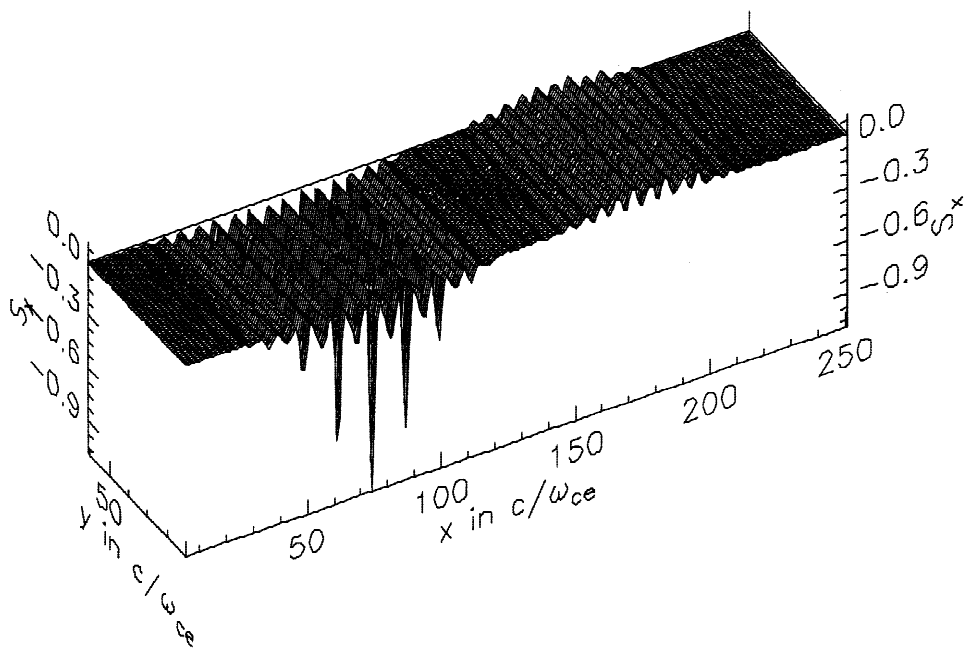


Fig. 5. Results of the same run as shown in Figure 2 but with a ten times stronger field strength ($E_{max} = m_e \omega c / e$). About 13% of the initial energy flux is transmitted, 61% reflected, and 26% absorbed. The transmitted part has the same shape and frequency as the initial pulse. The reflected part is distorted due to nonlinear interaction with the magnetized plasma.

energy flux here has dropped to about 2%, that is, much less than in the magnetized case. Similar cases with a relatively cold (0.5 keV) plasma showed transmission coefficients between 0.05 ($\omega_{ce} = 0$) and 1.5% ($\omega_{ce} = \omega_{pe}$).

It should be pointed out here that the transmission of the light energy is based on a linear theory. As a result, the transmitted light has the same properties as the incident light. In particular, unlike predicted by some other theories (Pegoraro *et al.*, 1997), the spectra of incident and transmitted pulse as well as the pulse shapes are similar to each other. This feature seems to coincide with the experimental observations (Giulietti *et al.*, 1997) of light transmission through overdense plasma.

Finally, we ran the same setup for nonlinear laser field strengths. The result for $E_{max} = m_e \omega c / e$ is shown in Figure 5. Even though our theory is not valid for these field strengths, the transmitted fraction of the electromagnetic field is almost identical to the linear case (Fig. 2 and Fig. 3) in shape, frequency, and relative amount of transmitted energy flux. The reflected part, not covered by our theory, becomes distorted and picks up different frequency components due to the nonlinear interaction with the magnetized plasma. It thus seems that the predictions made by the linear theory may be of interest to cases with the field strengths close to the experimental parameters used by Giulietti *et al.* (1997) and Fuchs *et al.* (1998).

Our conclusion is that the very high magnetic fields in the neighborhood of the focal spot of an intense laser incident on a solid target may produce a dramatic increase in the evanescence length of the wave fields in the high density plasma. This effect could be important in understanding the penetration of energy into the high density region and the particle acceleration processes which take place there. It is interesting to note that some recent experiments (Giulietti

et al., 1997; Fuchs *et al.*, 1998) have shown higher than expected transmission through thin foils. We cannot make any detailed comparison with the experiments, which have a much more complicated geometry than our simple model. In very thin foils, in particular, it is possible that the Larmor radius may be comparable to, or larger than the foil thickness. However, it is possible that modification of the wave properties by high magnetic fields may play some role.

ACKNOWLEDGMENT

This work was supported by the European Commission through the TMR Network SILASI, No. ERBFMRX-CT96-0043.

REFERENCES

- BEG, F.N. *et al.* (1996). *Phys. Plasmas* **4**, 447.
 BIRDSALL, C.K. & LANGDON, A.B. (1991). *Plasma Physics via Computer Simulations*, Adam Hilger.
 BORNATICI, M. *et al.* (1983). *Nucl. Fus.* **23**, 1153.
 FUCHS, J. *et al.* (1998). *Phys. Rev. Lett.* **80**, 2326.
 GIULIETTI, D. *et al.* (1997). *Phys. Rev. Lett.* **79**, 3194.
 MATTE, J.P. & AGUENAOU, K. (1992). *Phys. Rev. A* **45**, 2558.
 PEGORARO, F. *et al.* (1997). *Plasma Phys. Control. Fusion* **39**, B261.
 PERRY, M.D. & MOUROU, G. (1994). *Science* **264**, 917.
 SHKAROFSKY, I.P. (1966). *Phys. Fluids* **9**, 561, 570.
 SUDAN, R.N. (1993). *Phys. Rev. Lett.* **70**, 3075.
 TABAK, M. *et al.* (1994). *Phys. Plasmas* **1**, 1626.
 TAJIMA, T. (1989). *Computational Plasma Physics*, Addison-Wesley.
 TEYCHENNÉ, D. *et al.* (1998). *Phys. Rev. E* **58**, R1245.
 WILKS, S.C. *et al.* (1992). *Phys. Rev. Lett.* **69**, 1383.
 WILKS, S.C. *et al.* (1988). *Phys. Rev. Lett.* **61**, 337.
 WILKS, S.C. & KRUEER, W.L. (1997). *IEEE Journ. Quantum Elec.* **33**, 1954.